

# SINGLE PARTICLE SLOW DYNAMICS OF CONFINED WATER

Paola Gallo

*Dipartimento di Fisica, Università di Roma Tre and  
Istituto Nazionale per la Fisica della Materia, Unità di Ricerca Roma Tre,  
Via della Vasca Navale 84 I-00146 Roma, Italy.*

Molecular dynamics simulations of SPC/E water confined in a Silica pore are presented. The simulations have been performed at different hydration levels and temperatures to study the single-particle dynamics. Due to the confinement and to the presence of a hydrophilic surface, the dynamic behaviour of the liquid appears to be strongly dependent on the hydration level. On lowering temperature and/or hydration level the intermediate scattering function displays a double-step relaxation behaviour whose long time tail is strongly non-exponential. At higher hydrations two quite distinct subsets of water molecules are detectable. Those belonging to the first two layers close to the substrate suffer a severe slowing down already at ambient temperature. While the behaviour of the remaining ones is more resemblant to that of supercooled bulk SPC/E water. At lower hydrations and/or temperatures the onset of a slow dynamics due to the cage effect and a scenario typical of supercooled liquids approaching the kinetic glass transition is observed. Moreover, for low hydrations and/or temperatures, the intermediate scattering function clearly displays an overshoot, which can be assigned to the so called “Boson Peak”.

## I. INTRODUCTION

Water plays a most fundamental role on earth and its anomalous properties as a function of pressure and temperature are the subject of a longstanding scientific debate. Nevertheless there are still many crucial questions that remain to be answered. Some of the most important are described throughout all the present issue that is dedicated to metastable water [1]. In particular, the supercooled region has attracted a wide attention in the last few years. Thermodynamic as well as transport, dynamic, properties are not completely understood in this region. The main reason is that experimentally water can be supercooled only down to  $T_H \sim 236K$ . Then, because of homogeneous nucleation due to impurities, the liquid is driven toward the crystal phase [2]. Therefore studies of the liquid both through classic computer Molecular Dynamics, MD, and through theoretical models offer us ways to penetrate deep inside that region in the attempt to release the information that is not directly accessible to experiments.

In particular the normal limit of supercooling and the possibility of vitrification of water is a fundamental point that necessitates to be clarified. A recent experiment sustains the hypothesis that the amorphous phase can be connected to the normal liquid phase through a reversible thermodynamic path [3]. MD simulations of bulk supercooled SPC/E [4] water showed a kinetic glass transition as predicted by mode coupling theory (MCT) [5] at a critical temperature  $T_C \sim T_S$  [6], where  $T_S$  is the singular temperature of water [7], which is  $T_S = 228K$  or, for SPC/E, 49 degrees below the temperature of maximum density.

Within this framework a comparison of the behavior of the bulk liquid with the same liquid in a confined environment is highly interesting since both the phase

diagram and the dynamic behaviour of confined water could present an analogy with the same liquid in the bulk phase. The outcomings of this kind of researches can have therefore important experimental implication for the bulk. In particular experimentally forbidden regions of the phase diagram of bulk water could become accessible through the study of confined water. On the other hand a study of the modification of confined water with respect to the bulk is highly interesting for the development of both biological and industrial applications.

It has been inferred from experiments, although not conclusively proved, that confining water could be equivalent to the supercooling of the bulk [8,9]. In this paper I will inquire on how far this analogy can be pushed for SPC/E water confined in a silica pore and its bulk phase.

Among the different systems studied experimentally water confined in porous Vycor glass is one of the most interesting with relevance to catalytic processes and enzymatic activity. Vycor offers in fact to water a well characterized network of cylindrical pores, is composed of simple molecules  $SiO_2$ , has a quite well characterized structure with a sharp distribution of pore sizes with an average diameter of  $\sim 40 \pm 5 \text{Å}$ , i.e. the same order of magnitude of many biological confining environments, and a strongly hydrophilic inner surface. For these reasons several experiments on water-in-Vycor have been performed [9–11].

I shall show in the following the results concerning the single particle dynamics obtained from a series of MD simulations of SPC/E water confined in a cylindrical silica cavity [12–15]. The pore has been modeled to represent the average properties of Vycor pores. The simulated system from one side represents therefore a rather general confining environment and from the other offers the possibility of a direct comparison with experiments. The results shown in the following are focused on the role

of hydration level on slow dynamics of confined water in comparison with the bulk properties upon supercooling.

In the next section the details of the model of the pore are described together with the simulation details. In the third section the single particle dynamics of confined water is discussed in comparison with that of bulk SPC/E water. The last section concludes the paper with a discussion on the results.

## II. MODEL AND SIMULATION DETAILS

A single pore has been constructed for the simulations since in the range of timescales involved in this kind of dynamics water does not leak out of the pore. A cubic cell of vitreous  $SiO_2$  was built by melting a  $\beta$ -cristobalite single crystal and then by quenching the system down to ambient temperature [16,17]. The side of the cube is  $d \sim 70 \text{ \AA}$ . Inside the cell a cylindrical cavity, the pore, with diameter of  $40 \text{ \AA}$  was created by removing all the atoms lying within a distance of  $R = 20 \text{ \AA}$  from the  $z$ -axis passing through the center of the cube. The inner surface of the pore was then “corrugated” by removing from it all the  $Si$  atoms which were bonded to less than four  $O$ . At the surface oxygen atoms can be classified as bridging oxygens (bO) if they are bonded to at least two silicon atoms, non-bridging oxygens (nbO) otherwise. Then the dangling bonds of the nbO were saturated by attaching an hydrogen to each nbO. This procedure mimics the experimental preparation of the sample of water-in-Vycor in which internal surfaces of desiccated Vycor are hydrogenated before hydration. At the end of this process the cell contains 6400 silica atoms, 12500 bO and 230 nbO. This last number yields a surface density of acidic hydrogen of  $2.5 \text{ nm}^{-2}$  in good agreement with the  $2.3 \text{ nm}^{-2}$  obtained in the experiments [18]. The simulations have been performed in the NVE ensemble introducing water molecules into the pore. Water molecules interact among themselves via a SPC/E potential, and with Vycor atoms via an effective pair potential [16]. Both potentials have a Coulombic part plus a Lennard Jones term between oxygens. The parameters of the simulation are reported elsewhere [12,19]. The interactions cutoff is  $9 \text{ \AA}$  and the shifted force method has been used. For the Coulomb interaction it was checked that with respect to the correct use of the Ewald summation this technique was not producing qualitatively different results [12]. The timestep of the simulations was 2.5 fs. Equilibration, reached through a Berendsen thermostat [21], was monitored via the time dependence of the potential energy and the total energy. Along the pore axis ( $z$ -direction) periodic boundary conditions are applied to the water molecules. Along the remaining directions ( $xy$ ) water is confined. The glass is rigid.

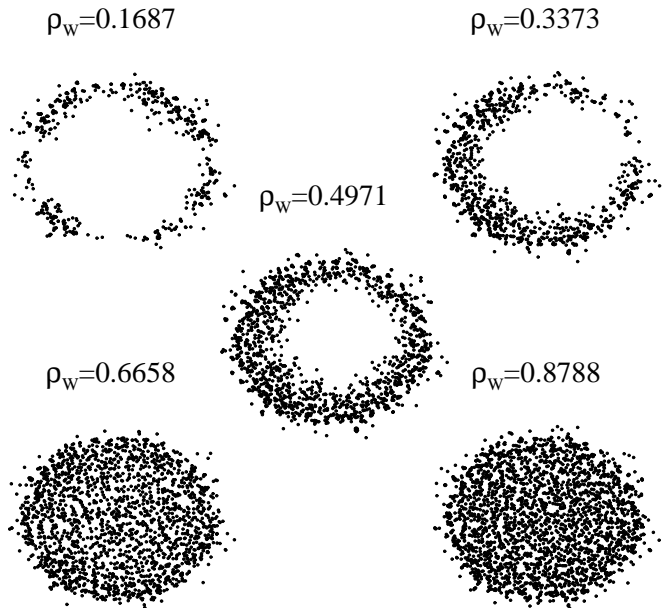


FIG. 1. Snapshots from simulations of SPC/E water inside a cylindrical cavity of diameter  $40 \text{ \AA}$  at ambient temperature. Only oxygens are shown.  $\rho_W$  is the global water density in  $g/cm^3$  (see Table I).

The molecular dynamics calculations have been performed for different numbers of water molecules, corresponding to different levels of hydration of the pore. The definition of hydration level of the pore deserves some consideration. Experimentally Vycor glass absorbs water up to 25% of its dry weight, this is defined as equilibrium or full hydration ( $h_f \simeq 0.25 \text{ g of water / g of Vycor}$ ). The experimental density of water when confined in such a pore at full hydration is estimated to be 11% less than its bulk value at ambient conditions i.e.  $\rho_W = 0.0297 \text{ molecules / \AA}^3 = 0.8877 \text{ g/cm}^3$  [20]. A partially hydrated sample is then experimentally obtained by absorption of water in the vapor phase until the desired level of hydration is reached. For the designed pore of this simulation the density of the full hydration is obtained for  $N_W = 2661$ , where  $N_W$  is the number of water molecules introduced in the pore. The five hydration levels investigated in the present work are reported in Table I. I will discuss here the results obtained for two temperatures:  $T = 298 \text{ K}$  and  $T = 240 \text{ K}$ .

TABLE I. Hydration levels of the pore.  $N_W$  is the number of water molecules and  $\rho_W$  the corresponding global density. <sup>(a)</sup>: based on estimated value for full hydration  $N_W = 2661$  molecules (see text).

$N_W$	% hydration <sup>(a)</sup>	$\rho_W \text{ (g/cm}^3\text{)}$
500	19%	0.1687
1000	38%	0.3373
1500	56%	0.4971
2000	75%	0.6658
2600	99%	0.8788

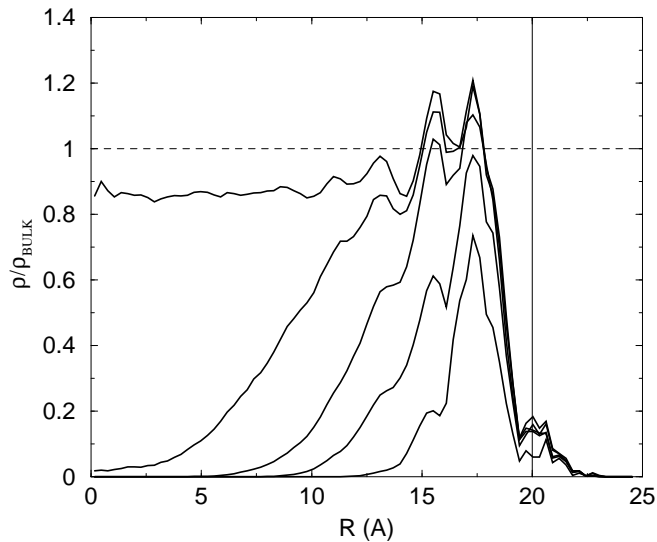


FIG. 2. Radial density profiles normalized to the bulk for oxygen atoms at ambient temperature for the five hydration levels investigated: first curve on the top corresponds to  $\rho_w = 0.8788 \text{ g/cm}^3$ , last on the bottom to  $\rho_w = 0.1687 \text{ g/cm}^3$ . The vertical line schematically indicates the pore surface. Right inside the pore the density is different from zero because few molecules are trapped in the pockets of the corrugated pore surface (see text).

The snapshots, see Fig.1, of the system at ambient temperature show that the simulated surface is strongly hydrophilic. At all the degree of hydration water adsorbs on the Vycor surface. A wide variety of water cluster is visible for the lowest global density investigated  $\rho_w = 0.1687 \text{ g/cm}^3$ , which is lower than the estimated monolayer coverage ( $\rho_w \simeq 0.2219 \text{ g/cm}^3$ ).

The density profiles of the oxygen atoms of confined water are shown in Fig.2. It is observed already at lower hydrations the presence of a layer of water molecules wetting the substrate surface. At nearly full hydration two layers of water with higher than bulk density are evident. Few molecules are trapped inside small pockets close to the surface, which are a byproduct of the “sample preparation process”. There is a strong tendency of water molecules close to the surface to form hydrogen bonds (HB) with the atoms of the substrate, in particular the hydrogens of water molecules with bO. As a consequence the HB network of water results to be strongly distorted close to the Vycor surface [12,14]. This is compatible with the findings of recent experiments on water-in-Vycor [11].

### III. SINGLE PARTICLE DYNAMICS OF CONFINED WATER

Bulk SPC/E water, like many glass forming liquid, when supercooled, or when the pressure is increased, develops a diversification of relaxation times scales, one

fast and one slow, well described by MCT [6]. In the MCT [5] scenario a liquid approaches the glass transition point with a dynamic behaviour mastered by the so called “cage effect”. The molecule or atom is trapped by the transient cage formed by its nearest neighbour,  $nn$ . After an initial ballistic regime it starts feeling the potential barrier of its  $nn$ . In this intermediate time region the particle is rattling in the cage formed by this potential barrier. When the cage relaxes the particle is free to move and enters the normal diffusive regime. But as the liquid gets closer to  $T_C$  the cage relaxation time becomes longer and eventually approaches infinity in the idealized MCT. Below  $T_C$  cages are frozen and only hopping processes can restore ergodicity allowing the particle to move (extended MCT) [22]. It is important here to stress that the cage effect is usually due in liquids to the increase of density, i.e. of  $nn$ , and in this respect water plays a peculiar role since there is no substantial increase in the number of  $nn$  on supercooling. It is the increased stiffness of the HB network at low temperature that allows for a “cage” to be formed also in bulk supercooled water.

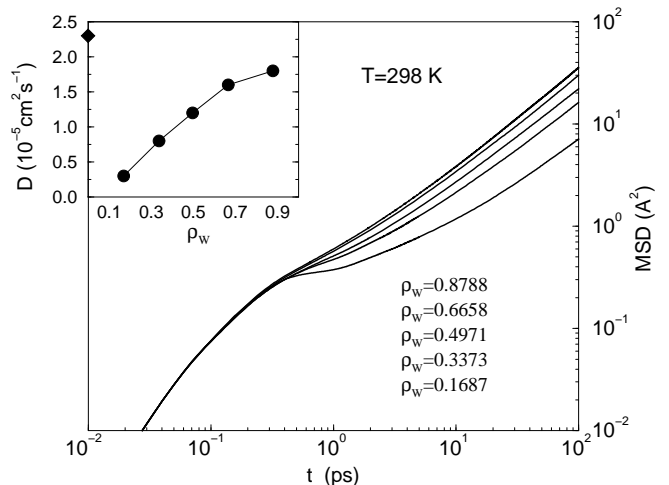


FIG. 3. MSD at ambient temperature of oxygens in the non-confined  $z$ -direction as a function of decreasing hydration from top to bottom. In the inset the diffusion coefficients are shown. They correspond to the various hydration levels (circles) and to bulk SPC/E water at ambient conditions (diamond).

Signatures of a behaviour à la Mode Coupling can be found in all the correlators that have an overlap with the density. In the following I will analyze for confined water in particular the mean square displacement, MSD, and the single particle density-density correlation function in the  $Q, t$  space also called the intermediate scattering function, ISF, or  $F_S(Q, t)$ . The signatures of this diversification of relaxation times and therefore the shouldering of the relaxation laws are more evident for the  $Q$  values close to the peak of the structure factor that for oxygen at ambient temperature is  $Q = 2.25 \text{ \AA}^{-1}$ . In particular the

long time tail of the ISF is predicted to have a stretched exponential behaviour when the system approaches the glass transition.

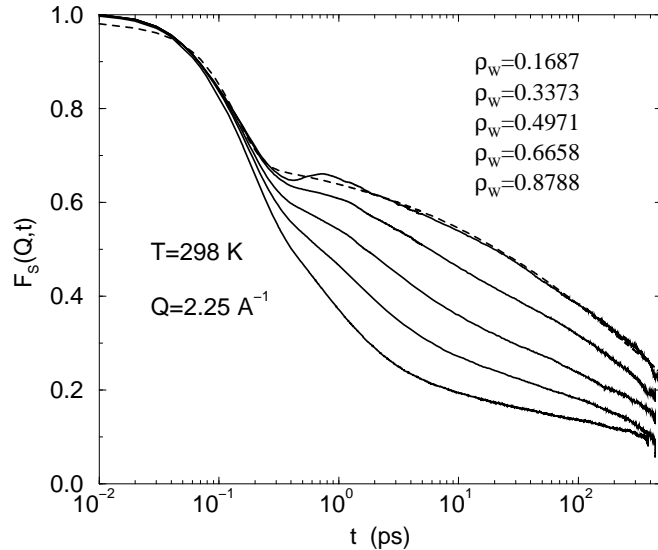


FIG. 4. ISF of oxygens at the peak of the structure factor in the confined xy direction. The highly non-exponential long time tail could be fitted (dashed line) to eq.1 only for the lower hydration.

In Fig.3 the mean square displacement of oxygens is displayed in the non-confined z-direction at ambient temperature as a function of hydration level. After the initial ballistic diffusion, before entering the diffusive regime, a flattening of the curve at intermediate times is observed as the hydration level is decreased. In the inset the bulk diffusion coefficient and the confined ones are displayed. There is a substantial decrease of average mobility as the hydration level in the pore is lowered. Correspondingly the oxygens ISF at the oxygen-oxygen peak of the structure factor, Fig.4, displays a shouldering of the relaxation laws upon decreasing hydration level. All the tails of the correlators of Fig.4 are highly non-exponential. Nonetheless these ISF could not be fitted to the same formula used for bulk supercooled water [6],

$$F_S(Q, t) = [1 - A(Q)] e^{-(t/\tau_s)^2} + A(Q) e^{-(t/\tau_l)^\beta} \quad (1)$$

except for the lowest hydration. In eq.1  $A(Q) = e^{-a^2 Q^2/3}$  is the Lamb-Mössbauer factor (the analogous of the Debye Waller Factor for the single particle) arising from the cage effect, and  $\tau_s$  and  $\tau_l$  are, respectively, the short and the long relaxation times. For the fit of the ISF of  $\rho_w = 0.1687 \text{ g/cm}^3$  shown in Fig.4 a cage radius  $a \simeq 0.44 \text{ \AA}$  is obtained, which is similar to the radius obtained for bulk supercooled water where  $a \simeq 0.5 \text{ \AA}$ . The lower radius obtained for confined water may be due to the slightly higher density of water close to the surface, see Fig.2. The short relaxation time  $\tau_s \simeq 0.14 \text{ ps}$  is again comparable to the bulk value which is  $\tau_s \simeq 0.2 \text{ ps}$ .

$\tau_l \simeq 356 \text{ ps}$  and  $\beta = 0.35$ . The  $\beta$  associated with  $\tau_l$  is very low compared to the typical values obtained for the supercooled bulk. Moreover the lowest hydration correspond to less than the monolayer coverage so that the dynamics of this system is that of clusters of water molecules attached to the pore surface. For the lowest hydration it is also observed a bump around  $0.7 \text{ ps}$  that could be possibly related to the existence of the Boson Peak feature in the  $S(q, \omega)$  [23]. This point will be discussed at the end of the paragraph. For the remaining correlators of Fig.4 no analytic function was found that could fit the strongly non-exponential tails. Due to the strong hydrophilicity of the pore a diversification of dynamic behaviour is to be expected as we proceed from the pore surface to the center of the pore. In Fig.5 the  $F_S(Q, t)$  for the highest global density at ambient temperature is split into the contribution coming from the two layers of water molecules closer to the pore surface, outer shells, and into the contribution coming from all the remaining ones, inner shells. The first two layers are defined according to the density profile, Fig.2. The inner shell contribution could be perfectly fit to eq.1 as shown in the figure, while the outer shells one decays to zero over a much longer timescale so that water molecules there behave already as a glass. From the fit it is extracted  $\beta = 0.74$ ,  $\tau_l = 0.75 \text{ ps}$ ,  $\tau_s = 0.21 \text{ ps}$ . The fit shows a remarkable agreement and both the  $\tau$  values are similar to those of bulk water, while for bulk water at ambient temperature  $\beta = 1$ . This kind of analysis has been extended for a different hydration and a different temperature.

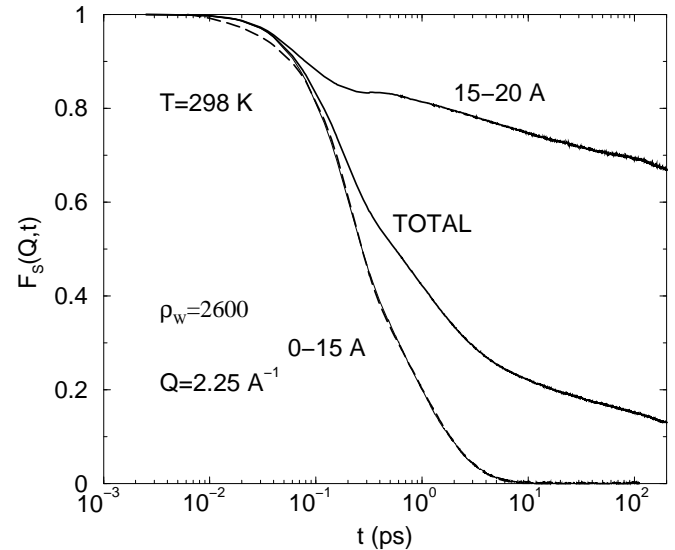


FIG. 5. ISF for oxygens at almost full hydration in the confined xy direction. Shell Analysis. The top curve is the contribution to the total ISF coming from the molecules in the two shells closest to the substrate, see Fig.2. The bottom curve is the contribution from the molecules in the remaining shells. The central one is the total ISF. The dashed line is the fit to eq.1.

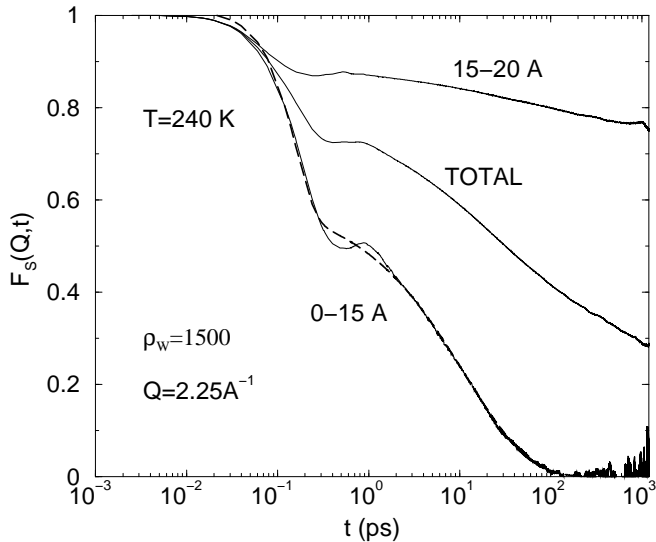


FIG. 6. Shell analysis for the supercooled regime. The dashed line is again the fit to eq. 1. Note that the bump related to the BP is now evident only for the inner shell contribution.

In Fig.6 the ISF shell analysis is shown at the peak of the structure factor for  $T=240$  K and  $\rho_W = 0.4971$   $g/cm^3$ . Also in this case the fit to the stretched exponential of the tail of the inner shells contribution is remarkable. From the fit  $\beta = 0.62$ ,  $\tau_l = 11$  ps  $\tau_s = 0.16$  ps are extracted. Again the  $\tau_l$  is similar to that of bulk water at the same temperature while the  $\beta$  here is much lower. In Fig.7 the  $\tau_l$  and the  $\beta$  values extracted from the fits to eq.1 done as a function of  $Q$  for  $T=240$  K and  $\rho_W = 0.4971$   $g/cm^3$  are shown. The  $\beta$  value reaches a plateau value and the  $\tau_l$  values show a  $Q^2$  dependence. Both these behaviours are typical of a glass former undergoing a kinetic glass transition and in particular the  $Q^2$  behaviour has been observed for example in glycerol close to the glass transition [24].

Let us now come back to Fig.4 where for the lowest hydration a bump around 0.7 ps is clearly visible. Deeply supercooled bulk water displayed the same peak around 0.35 ps [6,25]. This overshoot has been observed in simulations of supercooled strong glass formers like  $SiO_2$  [23]. It has been attributed in literature to the existence of a Boson Peak (BP) in the frequency domain. The BP is an excess of vibrational modes present in many glasses. When this glassy anomaly appears in the liquid state it is considered as precursor of the glass transition. This peak in the ISF has been also alternatively related to a disturbance propagating in a finite box. If there are periodic boundary conditions imposed (z direction for the present system) the disturbance would reenter the box after  $t = L/v_s$  where  $v_s$  is the sound velocity [26]. In spite of the possible existence of this finite size effect it has been recently proven that the BP can be detected by MD [23].

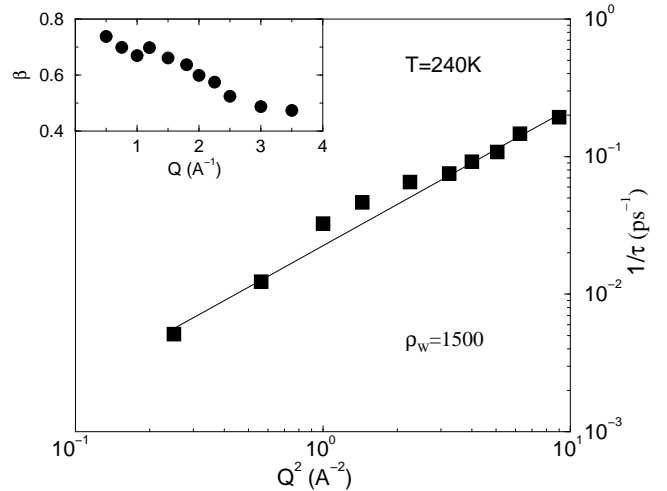


FIG. 7.  $\tau_l$  (main picture) and  $\beta$  (inset) values extracted from the fit of the long time tail of the ISF to eq.1. The continuous line has slope 2. The  $Q^2$  behaviour has been found in glass formers close to the glass transition.

Note that in this system the same bump is present also in the supercooled confined simulation, see Fig.6, and it is more evident for the inner shells. So that the presence of a disordered surface from one side seems to enhance the temperature at which the BP shows up and also its intensity with respect to the bulk. From the other side since the silica glass is rigid in our simulation the water molecules in contact with the glass cannot vibrate much so that practically only the inner shells can sustain vibrations. In Fig.8 same correlators of Fig.6 in the xy and z direction are shown. It is important to stress here that for this system the finite size effect in the xy directions is a feature also of the real pore.

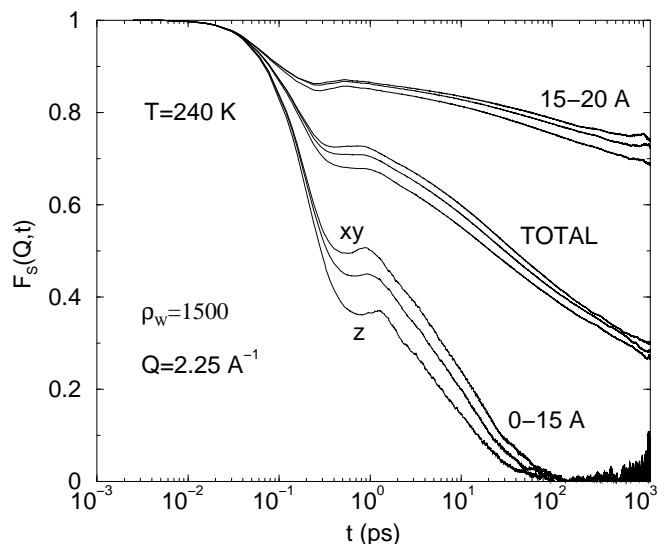


FIG. 8. Shell analysis for the supercooled regime in the confined (xy), non confined (z) and in an average random direction (central curve in each group of three). In particular: ISF from the two shells closest to the substrate (top curves), inner shells (bottom curves) and total (central curves).

This bump is therefore likely to be observed for water-in-Vycor. Both for the  $t$  corresponding to the minima and the maxima of the bump appearing in the lowest curves of Fig.8 the ratio of the  $t_z/t_{xy}$  is 1.44 against the 1.75 of the ratio between the lengths of the pore  $L_z = 70\text{\AA}$  and  $L_{xy} = 40\text{\AA}$ . Moreover, although less evident, a BP can be observed also for the outer shells in Fig.8 and the location is completely different with respect to that of the inner shells. So that in our ISFs there is no direct quantitative connection with a finite size effect that can be detected from the shape and the location of these bumps. It can be inferred from these data that both the size and the geometry, and the presence of surface strongly influence the nature of this peak. Size and geometry signatures can be seen in the change of location of the peak in the ISF in xy and z directions, see Fig.8. Signatures of a presence of a hydrophilic rigid surface can be related to the fact that the bump is more evident for the inner shells and is present already at room temperature. The changes of location and shape with respect to the bulk are therefore also probably influenced by all these causes. None-the-less, no quantitative statements can be made at this stage. Therefore both a frequency domain analysis and a instantaneous normal mode analysis can help to shed light on this issue and they are currently in progress on this system.

#### IV. DISCUSSION AND CONCLUSIONS

The results discussed in this paper show that for SPC/E water model an analogy between the supercooled bulk and the confined as a function of hydration level of the pore is possible only to the extent that in confined water upon decreasing the hydration level a glassy behaviour appears already at ambient temperature while for bulk water supercooling is required. None-the-less the manner the confined liquid approaches the kinetic glass transition temperature appears completely different. In the pore at higher hydration levels, due to the hydrophilic surface, two quite distinct subsets of water molecules are detectable. Experiments in favour of two phases for confined hydrogen bonded liquids are present in literature [27]. The subset that is in contact with the surface is at higher density with respect to the bulk and is already a glass with low mobility even at ambient temperature. The inner subset displays, like a supercooled liquid, a two step relaxation behaviour à la MCT. It behaves none-the-less differently from the supercooled bulk. In fact it turns out that confined and bulk relaxation times are compa-

rable at the same temperatures but the  $\beta$  values of the confined water are much lower than those of the bulk always at the same temperature. About the so called Kolhraush exponent  $\beta$  can be said that in general it is different for different systems but apparently no special significance can be attributed to its numerical value [5]. It is also important to mention here that SPC/E potential is considered one of the best potential for water upon supercooling, but these features are not produced by all potentials. For example the ST2 shows a “jump diffusion” behaviour upon supercooling [28]. These two potential in particular are known to sandwich the behaviour of experimental water so that ST2 water is less and SPC/E water is more structured than real water. On the other hand experimental signatures of MCT behaviour have been found both in the bulk [29] and in water-in-Vycor [8,9] and also experimental signatures of a possible existence of a BP [30] in water-in-Vycor have been detected. These results are encouraging and more simulations on this pore as a function of temperature and hydration are in progress for a full MCT test and a complete comparison with the bulk.

#### V. ACKNOWLEDGEMENTS

I wish to thank Mauro Rovere, Maria Antonietta Ricci and Eckhard Spohr for their contributions to this work, C. Austen Angell, Burkhard Geil, Alberto Robledo and Francesco Sciortino for stimulating discussions on topics related to this paper.

- 
- [1] For a review on metastable liquids an water in particular see: P. G. Debenedetti, *Metastable Liquids: Concepts and Principles* (Princeton University Press, Princeton, 1997).
  - [2] C. A. Angell *Ann. Rev. Phys. Chem.*, 1983, **34**, 593.
  - [3] Robin J. Speedy, Pablo G. Debenedetti, Scott R. Smith, C. Huang, Bruce D. Kay, *J. Chem. Phys.*, 1996, **105** 240.
  - [4] H. J. C. Berendsen, J. R. Grigera and T. P. Straatsma, *J. Phys. Chem.*, 1987, **91**, 6269.
  - [5] W. Götze and L. Sjögren, *Rep. Prog. Phys.*, 1992, **55**, 241.
  - [6] P. Gallo, F. Sciortino, P. Tartaglia and S.-H. Chen, *Phys. Rev. Lett.*, 1996, **76**, 2730; F. Sciortino, P. Gallo, P. Tartaglia, S.-H. Chen, *Phys. Rev. E*, 1996, **54**, 6331.
  - [7] R. J. Speedy and C. A. Angell, *J. Chem. Phys.*, 1976, **65**, 851.
  - [8] S.-H. Chen, P. Gallo and M. C. Bellissent-Funel *Can. J. Phys.*, 1995, **73**, 703.
  - [9] J.-M. Zanotti, M.-C. Bellissent-Funel and S.-H. Chen, *Phys. Rev. E*, 1999, **59**, 3084.

- [10] For a review see on experimental study of water-in-Vycor see: S.-H. Chen and M.-C. Bellissent-Funel in *Hydrogen Bond Networks*, edited by M.-C. Bellissent-Funel and J. C. Dore, NATO ASI Series C: Mathematical and Physical Science, **435**, 337 (Kluwer Academic Publishers, 1994).
- [11] F. Bruni, M. A. Ricci, and A. K. Soper, *J. Chem. Phys.*, 1998, **109**, 1478; A. K. Soper, F. Bruni and M. A. Ricci, *J. Chem. Phys.*, 1998 **109**,1486.
- [12] E. Spohr, C. Hartnig, P. Gallo and M. Rovere, *J. Mol. Liq.*, 1999, **80**, 165.
- [13] P. Gallo, M. A. Ricci, M. Rovere C. Hartnig, E. Spohr, *Europhys. Lett.*, 2000, **49**, 183 .
- [14] C. Hartnig, W. Witschel, E. Spohr, P. Gallo, M. A. Ricci and M. Rovere, *J. Mol. Liq.*, 2000, in press.
- [15] P. Gallo, M. Rovere, M.A. Ricci, C. Hartnig, E. Spohr, *Phylosoph. Mag. B*, 1999, **79**, 1923.
- [16] A. Brodka, and T. W. Zerda, *J. Chem. Phys.*, 1996, **104**, 6319.
- [17] B. P. Feuston and S. H. Garofalini, *J. Chem. Phys.*, 1988, **89**, 5818.
- [18] Y. Hiramata, T. Takahashi, M. Hino, and T. Sato, *J. Colloid Interface Sci.*, 1996, **184**, 349.
- [19] M. Rovere, M. A. Ricci, D. Vellati and F. Bruni, *J. Chem. Phys.*, 1998, **108**, 9859.
- [20] M. J. Benham, J. C. Cook, J. C. Li, D. K. Ross, P. L. Hall and B. Sarkissian, *Phys. Rev. B*, 1989, **39**, 633.
- [21] H. J. C. Berendsen, J. P. M. Postma, W. F. van Gunsteren, A. Di Nola, and J. R. Haak, *J. Chem. Phys.*, 1984, **81**, 3684.
- [22] W. Götze and L. Sjögren, in *Transport theory and statistical physics*, 1995, **24**, 801.
- [23] J. Horbach, W. Kob, K. Binder, and C. A. Angell, *Phys. Rev. E*, 1996, **54**, R5897; J. Horbach, W. Kob, and K. Binder, to appear in the proceedings of *Neutrons and numerical methods*, 1998 Grenoble, Ed. H.G. Buttner et Al..
- [24] W. Petry and J. Wuttke, in *Transport theory and statistical physics*, 1995, **24**, 1075.
- [25] S.-H. Chen, P. Gallo, F. Sciortino, P. Tartaglia, *Phys. Rev. E*, 1997, **56**, 4231.
- [26] L.J. Lewis adn G. Wahnström, *Phys. Rev. E*, 1994, **50**, 3865.
- [27] Yu. B. Mel'nichenko, J. Schüller, R. Richert, and B. Ewen, C. K. Loong, *J. Chem. Phys.*, 1995, **103**, 2016.
- [28] Dietmar Paschen and Alfons Geiger, *J. Phys. Chem. B*, 1999, **103** 4139.
- [29] F.X. Prielmeir, E.W. Lang, R.J. Speedy and H.D. Lüdemann, *Phys. Rev. Lett.* 1987, **59** 1128; C.A. Angell *Nature*, 1988, **331**, 206; A.P. Sokolov, J. Hurst, and D. Quitmann, *Phys. Rev. B*, 1995, **51** 12865.
- [30] A. R. Bizzarri, F. Bruni, S. Cannistraro, M. A. Ricci, 1999, private communication.